

# Defective RAB1B-related megakaryocytic ER-to-Golgi transport in RUNX1 haploinsufficiency: impact on von Willebrand factor

Gauthami Jalagadugula,<sup>1</sup> Lawrence E. Goldfinger,<sup>1,2</sup> Guangfen Mao,<sup>1</sup> Michele P. Lambert,<sup>3</sup> and A. Koneti Rao<sup>1,4</sup>

<sup>1</sup>Sol Sherry Thrombosis Research Center and <sup>2</sup>Department of Anatomy and Cell Biology, Lewis Katz School of Medicine at Temple University, Philadelphia, PA; <sup>3</sup>Department of Pediatrics, Children's Hospital of Philadelphia and University of Pennsylvania, Philadelphia, PA; and <sup>4</sup>Department of Medicine, Lewis Katz School of Medicine at Temple University, Philadelphia, PA

## Key Points

- GTPase *RAB1B* is a direct transcriptional target of RUNX1 in MK/platelets and is down-regulated in *RUNX1* haploinsufficiency.
- *RUNX1* down-regulation is associated with defective RAB1B-related ER-to-Golgi transport and alterations in  $\alpha$ -granule vWF.

Patients with RUNX1 haploinsufficiency have thrombocytopenia, platelet dysfunction, and deficiencies of  $\alpha$ -granules and dense granules. Platelet expression profiling of a patient with a heterozygous *RUNX1* mutation (c.969-323G>T) revealed decreased *RAB1B*, which encodes a small G protein. RAB GTPases regulate vesicle trafficking, and RAB1B is implicated in endoplasmic reticulum (ER)-to-Golgi transport in nonhematopoietic cells, but its role in megakaryocytes (MK) is unknown. We addressed the hypothesis that *RAB1B* is a transcriptional target of RUNX1 and that RAB1B regulates ER-to-Golgi transport in MK cells. Chromatin immunoprecipitation studies and electrophoretic mobility shift assay using phorbol 12-myristate 13-acetate (PMA)-treated human erythroleukemia cells revealed RUNX1 binding to *RAB1B* promoter region RUNX1 consensus sites, and their mutation reduced the promoter activity. *RAB1B* promoter activity and protein expression were inhibited by *RUNX1* siRNA and enhanced by RUNX1 overexpression. These indicate that *RAB1B* is a direct RUNX1 target, providing a mechanism for decreased *RAB1B* in patient platelets. Vesicle trafficking from ER to Golgi in PMA-treated human erythroleukemia cells was impaired along with Golgi disruption on siRNA downregulation of *RUNX1* or *RAB1B*. The effects of *RUNX1* knockdown were reversed by *RAB1B* reconstitution. Trafficking of von Willebrand factor (vWF), an  $\alpha$ -granule MK synthesized protein, was impaired with *RUNX1* or *RAB1B* downregulation and reconstituted by ectopic RAB1B expression. Platelet vWF was decreased in patients with *RUNX1* mutations. Thus, ER-to-Golgi transport, an early critical step in protein trafficking to granules, is impaired in megakaryocytic cells on *RUNX1* downregulation, secondary to decreased *RAB1B* expression. Impaired *RAB1B* mediated ER-to-Golgi transport contributes to platelet  $\alpha$ -granule defects in *RUNX1* haploinsufficiency.

## Introduction

RUNX1 (also called AML1 or CBFA2) is a hematopoietic transcription factor that plays a major role in definitive hematopoiesis, megakaryopoiesis, and platelet production.<sup>1,2</sup> *RUNX1* haploinsufficiency is associated with familial thrombocytopenia, platelet dysfunction,  $\alpha$ -granule and dense granule deficiencies, impaired secretion of granule contents, and predisposition to acute leukemia.<sup>1,3-5</sup> Little is known regarding the mechanisms leading to deficiencies in the granules and their cargoes in patients with RUNX1 haploinsufficiency. It is likely that multiple mechanisms contribute to the platelet functional defects.<sup>4</sup> In previous studies in a patient with RUNX1 haploinsufficiency, we reported the presence of thrombocytopenia, abnormalities in  $\alpha$  and dense granules, and impaired aggregation, secretion,

phosphorylation of pleckstrin and myosin light chain, and activation of GPIIb-IIIa on platelet receptor activation.<sup>6-9</sup> Platelet expression profiling of this patient using Affymetrix microarrays showed that several genes were downregulated,<sup>7</sup> and we have shown that some of the genes are direct transcriptional targets of RUNX1.<sup>8,10-13</sup> Profiling studies further showed downregulation of *RAB1B*,<sup>7</sup> which encodes the Ras-related small GTPase RAB1B, which is intimately involved in vesicle transport of proteins from endoplasmic reticulum (ER) to the Golgi compartment, a central organelle in the secretory pathways.<sup>14-17</sup> This is a critical step in the trafficking of proteins synthesized in the ER to their final location in specific platelet granules. In eukaryotic cells, the major players in the secretory and endocytic pathways leading to formation of distinct vesicles/granules bearing different cargoes include the ER, the ER-Golgi intermediate compartment, the Golgi and its subcompartments, and the different classes of endosomes, lysosomes, and regulated secretory granules.<sup>18</sup> Rab proteins regulate specific steps in membrane trafficking, including in vesicle formation and movement, and in membrane fusion.<sup>18</sup> These GTPases shuttle between GTP-bound (active) and GDP-bound (inactive) forms to regulate their binding to downstream effectors and execute cellular functions.

Little is currently known regarding the role of *RAB1B* in platelets or megakaryocytes (MK). Previous studies implicating *RAB1B* in ER-to-Golgi trafficking have been performed in HeLa cells<sup>14,15,17</sup> or CHO cells.<sup>16</sup> Neither of these is of hematopoietic origin, and HeLa cells do not express RUNX1.<sup>19</sup> On the basis of the findings in our patient with RUNX1 haplodeficiency, we pursued the hypothesis that *RAB1B* is a transcriptional target of RUNX1 and that downregulation of *RAB1B* or *RUNX1* is associated with defective ER-to-Golgi transport in megakaryocytic cells. These studies provide evidence that RUNX1 regulates via RAB1B, which is essential for ER-to-Golgi transport, an early event in protein trafficking that governs  $\alpha$ -granule formation and contents. Our studies show that RUNX1 haplodeficiency alters trafficking of vWF and platelet vWF levels.

## Patients and methods

### Patient information

The initial patient (P1) studied has thrombocytopenia and abnormal platelet function associated with a single point mutation (c.969-323G>T) in intron 3 at the splice acceptor site for exon 4, leading to a frame shift with premature termination in the conserved RUNT homology domain of *RUNX1*.<sup>9</sup> Details of the platelet function abnormalities<sup>6,7,9</sup> and expression profiling studies in this patient<sup>7</sup> have been previously described.

Studies were performed in 2 patients from a second family (8-year-old male, P2, and his 3-year-old sister, P3) with thrombocytopenia and a *RUNX1* mutation (c.508+1G>A). The maternal grandmother and great uncle had history of acute myeloid leukemia. This patient had abnormal agonist-induced aggregation and secretion on laboratory testing. The studies on the patients and control subjects were approved by institutional review boards of the Lewis Katz School of Medicine at Temple University and the Children's Hospital of Philadelphia, and were performed after obtaining the informed consent. The studies were conducted following the guidelines of the Helsinki Declaration.

### Immunofluorescence studies

Platelets from the patients and healthy controls or human erythroleukemia (HEL) cells were treated as described for each

study and then seeded on coverslips precoated with human plasma fibronectin and fixed and imaged by epifluorescence and confocal microscopy as described.<sup>8</sup> Images were acquired on a Nikon E1000 microscope or Leica TCS SP5 confocal microscope, using a 63 $\times$ /1.40 n.a. oil immersion objective at room temperature and Q Capture or Leica imaging software, respectively. Postacquisition processing and analysis was performed with Adobe Photoshop and ImageJ, and was limited to image cropping and brightness/contrast adjustments applied to all pixels per image simultaneously. Fluorophores used were fluorescein isothiocyanate or Cy3.

### Cell culture

HEL cells from American Type Cell Culture (Rockville, MD) were grown and induced in RPMI-1640 medium as described.<sup>20</sup>

### Real-time PCR

Total RNAs from platelets isolated from whole blood of healthy donors and the patient<sup>8</sup> were subjected to first-strand cDNA synthesis using Superscript III (Applied Biosystems) and amplified by real-time polymerase chain reaction (PCR) by SYBR Green PCR mix, using primers (supplemental Table 1) for *RAB1B*, *RAB1A*, and *GAPDH* (0.1  $\mu$ M each). The parameters used for real-time PCR were as follows: 95°C for 10 minutes followed by 40 cycles of 95°C for 15 seconds, 55°C for 20 seconds, and 72°C for 20 seconds, using a Master Cycler Real-Time PCR system (Eppendorf, Hauppauge, NY), and relative abundances were calculated by the  $\Delta\Delta C_T$  method, using *GAPDH* as the reference gene.

### Chromatin immunoprecipitation assay

Chromatin immunoprecipitation (ChIP) assays were performed on HEL cells ( $1 \times 10^8$ ) treated with phorbol 12-myristate 13-acetate (PMA; 10 nM) for 24 hours, using the ChIP-It kit (Active Motif, Carlsbad, CA) and antibodies as described.<sup>10</sup> Chromatin samples were immunoprecipitated with anti-RUNX1 antibody (sc-8563x) or with normal immunoglobulin G (IgG; sc-2028; Santa Cruz, Dallas, TX). Immunoprecipitated samples were analyzed by PCR, using the primers shown in supplemental Table 2. Amplification was performed using Go Taq Green Master Mix with 1 cycle at 95°C for 2 minutes, followed by 32 cycles of 95°C for 30 seconds, 62°C for 45 seconds, and 72°C for 60 seconds.

### Electrophoretic mobility shift assays

Electrophoretic mobility shift assays (EMSA) were performed using HEL cell nuclear extracts as described.<sup>20</sup> *RAB1B* promoter region –785/–1 (from ATG) has 4 RUNX1 consensus sites. Oligonucleotides encompassing these sites (RAB1B site 1 probe –445/–426, site 2 probe –630/–611, site 3 probe –659/–640, and site 4 probe –778/–759) were labeled with infrared dye 700 (LI-COR Biosciences, Lincoln, NE; supplemental Table 3). Supershift assays were performed with anti-RUNX1 antibody (sc-8563x) or normal IgG (sc-2028; Santa Cruz). Gels were visualized on Odyssey Infrared Imaging System (LI-COR Biosciences).

### Promoter-reporter assays

The *RAB1B* wild-type (WT) promoter (–785/+15) and constructs with specific mutations in RUNX1 consensus sites were generated by directional PCR method, using gene-specific primers incorporated with restriction sites (Xho I at 5' side and Hind III at 3' side). The PCR products were cloned into the TOPO TA cloning vector. The recombinant TOPO TA plasmid was digested with appropriate restriction enzymes, and the promoter region was subcloned

between the same restriction sites of the pGL3-Basic promoter. The sequences were confirmed by DNA sequencing on the ABI Prism 377 (Applied Biosystems).

Promoter-reporter constructs were transfected individually along with a standard Renilla luciferase (in 50:1 ratio) into HEL cells ( $2 \times 10^6$ ), using Lipofectamine 2000 (Thermo Fisher Scientific, Philadelphia, PA). The primer sequences of WT construct and its mutants are shown in supplemental Table 4. Dual-luciferase assays were performed as described.<sup>20</sup> Promoter activity was expressed as the ratio of firefly luciferase activity to Renilla luciferase activity, relative to that of the promoter-less vector. All experiments were performed 3 times in triplicate.

### RUNX1 downregulation and overexpression

HEL cells ( $2 \times 10^6$ ) were cotransfected with WT *RAB1B* luciferase construct, along with control siRNA or *RUNX1* siRNA (100 nM each; Santa Cruz) to study the effect of downregulation of these genes. To study the effect of *RUNX1* overexpression, cells ( $2 \times 10^6$ ) were cotransfected with *RAB1B* WT luciferase construct or its mutants, along with *RUNX1* expression vector, *RUNX1*-pCMV6-XL4, or its empty expression vector, pCMV6-XL4 (1  $\mu$ g each; Origene Technologies, Rockville, MD). pRL-TK (Renilla luciferase) plasmid was also used in each transfection as an internal standard, and dual-luciferase assays were performed as described here. HEL cell lysates were prepared and immunoblotted using antibodies against *RUNX1*, *RAB1B*, and actin or GAPDH.<sup>10</sup>

### Immunoblotting

Human platelets and HEL were lysed in a M-Per protein extraction reagent (Pierce Biotechnology) supplemented with a protease inhibitor cocktail (Active Motif, Carlsbad, CA). Cell lysates (20  $\mu$ g) were subjected to 4% to 20% Mini-PROTEAN TGX gels (Bio-Rad, Hercules, CA), and the protein was transferred to PVDF membrane (Millipore, Billerica, MA) and was probed with antibodies against *RAB1B* (sc-599), *RUNX1* (sc-8563 or sc-365644), actin (sc-1616R; Santa Cruz, CA), or von Willebrand Factor (vWF; ab6994; Abcam, Cambridge, MA). The blots were probed with IR Dye-labeled secondary antibodies (LI-COR Biosciences), using the Odyssey Infrared Imaging System (LI-COR Biosciences).

### ER-to-Golgi transport studies

ER-to-Golgi transport was studied using vesicular stomatitis virus G (VSVG) envelope glycoprotein tagged with enhanced GFP, as described by Presley et al<sup>21</sup> with modifications. PMA-treated (10 nM, 24 hours) HEL cells ( $1 \times 10^6$ ) were nucleofected with VSVG-GFP and E2-Crimson-GALT-CFP plasmids (1  $\mu$ g each), along with control siRNA or *RAB1B* siRNA or *RUNX1* siRNA (100 nM each), or *RUNX1* siRNA + 2  $\mu$ g of *RAB1B* expression plasmid (Origene Technologies, Rockville, MD), using Amaxa cell line Nucleofector kit V in a nucleofector 2b device (Lonza Company). These cells were resuspended in the medium supplemented with 10 nM PMA and incubated at 37°C with 5% CO<sub>2</sub>. After 24 hours, cells were resuspended by centrifugation in fresh medium with 10 nM PMA, transferred onto fibronectin-coated plates, and incubated at 40°C for 12 to 15 hours, followed by incubation at 32°C for 30 minutes. The cells were then fixed and imaged by confocal microscopy, followed by calculation of the Pearson's correlation coefficient from at least 100 cells per condition, as described.<sup>8,22</sup> VSVG cDNA sequence was isolated by restriction digestion from pEGFP-VSVG vector (Addgene 11912, deposited by Jennifer Lippincott-Schwartz) purchased from Addgene

(a plasmid repository; Cambridge, MA) and cloned into pEGFP-C3 vector (Takara Bio, Mountain View, CA). GALT-CFP plasmid was prepared as follows: E2-Crimson-tagged  $\beta$ 1, 4 galactosyltransferase 1 (GalT) with KDEL ER targeting sequence deleted was created in the pECFP vector by subcloning the E2-Crimson cassette in place of enhanced cyan fluorescent protein cassette in the GALT-CFP plasmid (Addgene 11937, a gift from Jennifer Lippincott-Schwartz)

### Bioinformatics

*RAB1B* sequence (accession no. NM\_030981.2) was obtained from the National Center for Biotechnology Information gene database. Potential binding sites for transcription factors were analyzed using the computer program TFBIND (<http://tfbind.hgc.jp>).

### Statistical analysis for in vitro studies

Results of the in vitro studies are expressed as mean  $\pm$  standard error of the mean (SEM). Differences were compared using the Student *t* test.

## Results

### Decreased platelet *RAB1B* expression in *RUNX1*-haplodeficiency

Platelet expression profiling revealed that *RAB1B* is decreased in the patient with *RUNX1* haplodeficiency (fold change, 0.318; *P* = .025) compared with platelets from 6 healthy control participants, using Affymetrix U133 Gene Chips.<sup>7</sup> This was validated by quantitative PCR (Figure 1A). Immunofluorescence studies using anti-*RAB1B* antibodies showed that *RAB1B* protein expression was decreased in platelets from our first patient, P1, compared with healthy participants (Figure 1B). Studies in 2 siblings, patients P2 and P3, from an unrelated family with a *RUNX1* mutation also showed platelet *RAB1B* mRNA was decreased (Figure 1C), with decreased platelet *RAB1B* protein on immunofluorescence studies (Figure 1D). On immunoblotting, platelet *RAB1B* was lower in the patients compared with control subjects (Figure 1E).

### *RUNX1* regulates *RAB1B*

*RAB1B* promoter sequence revealed 4 *RUNX1* consensus binding sites within 800 bp from the ATG codon: at -440/-435 (site 1), -622/-617 (site 2), -660/-655 (site 3), and -770/-765 (site 4; Figure 2A). The ChIP assays were performed on HEL cell chromatin, using an anti-*RUNX1* antibody. PCR amplification of the immunoprecipitated chromatin showed enrichment of promoter regions with site 1 and site 4 by anti-*RUNX1* antibody, and no enrichment was noted with normal IgG. The promoter fragments containing site 2 and site 3 were not enriched (Figure 2A). These results indicate that *RUNX1* binds in vivo to *RAB1B* promoter.

EMSA were performed using HEL nuclear extracts and labeled *RAB1B* oligos containing each of the *RUNX1* consensus sites (supplemental Table 2). Because of the proximity of sites 2 and 3 (Figure 2A), a single probe encompassing both sites was used in these studies. These studies revealed that *RUNX1* was present in complex with consensus sites 1 and 4 (Figure 2B), but not with sites 2 and 3 (data not shown), a result similar to that with ChIP analysis. In studies with the oligo containing site 1 (Figure 2B), there was protein binding (Figure 2B, lane 2), which was competed with excess unlabeled oligo (lane 3). There was no alteration in binding by normal IgG (lane 4), but it was inhibited by *RUNX1* antibodies (lane 5). Similar results were

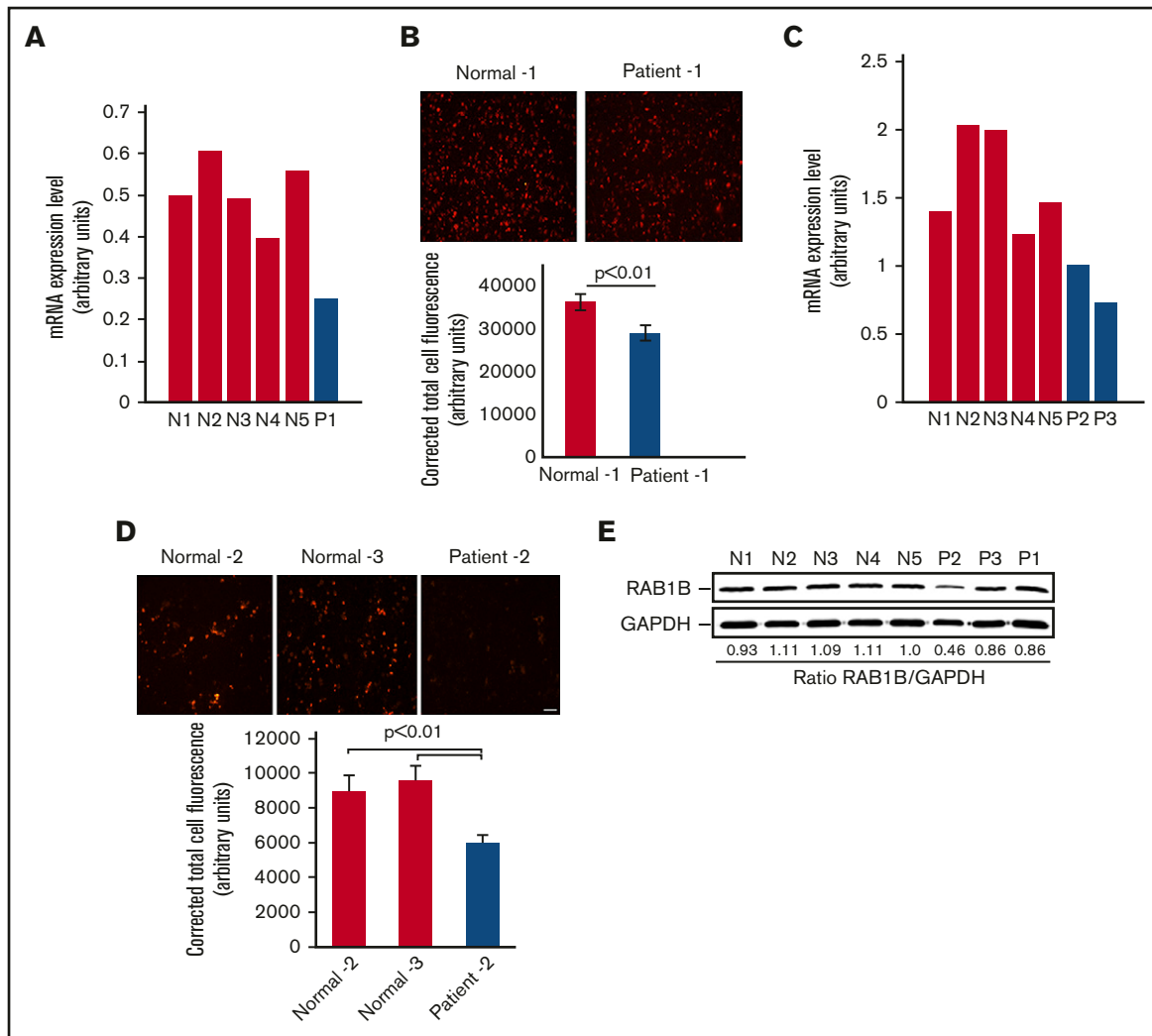


**Figure 1. *RAB1B* expression in platelets from the patients with *RUNX1* haploinsufficiency and healthy control subjects.** (A) Platelet *RAB1B* mRNA levels in the index (P1) patient and 5 normal subjects (N1-N5) by quantitative PCR. Shown are mRNA levels normalized to GAPDH. (B) Immunofluorescence studies of platelet *RAB1B* expression in the index patient P1 and a normal subject. Platelets were labeled with *RAB1B* polyclonal antibody, detected with fluorescein isothiocyanate (pseudocolored red)-conjugated secondary antibody, and imaged on a Nikon E1000 microscope. Corrected total cell immunofluorescence is shown  $\pm$  SEM. (C) Platelet *RAB1B* mRNA in 2 siblings (P2 and P3) from a second family with *RUNX1* mutation and 5 normal subjects (N1-N5). (D) Platelet *RAB1B* immunofluorescence in patient P2 and 2 normal subjects. Bar, 10  $\mu$ m (scale also applies to panel B). Corrected total cellular fluorescence is shown  $\pm$  SEM. The *P* values represent comparisons of the patient with each of the control subjects. (E) Platelet *RAB1B* by immunoblotting in 3 patients (P1-P3) and 5 healthy subjects (N1-N5). Also shown is the ratio of *RAB1B* to GAPDH.

observed in studies of oligo with site 4. Together, the ChIP and EMSA studies revealed *RUNX1* binding to sites 1 and 4. In promoter-reporter studies using constructs with *RAB1B* promoter region (Figure 2C), mutations in site 1 or site 4 resulted in marked reduction in promoter activity, but no change was noted in reporter activities with specific mutations in sites 2 or 3. Together, these findings indicate that *RUNX1* binds to sites 1 and 4 in the *RAB1B* promoter region, and that these sites are functional.

*RUNX1* overexpression in HEL cells increased *RAB1B* protein expression (Figure 3A) and *RAB1B* promoter activity of the WT construct (Figure 3B). The increase in promoter activity was abolished when *RUNX1* binding sites 1 and 4 (but not sites 2 and 3) were mutated individually (Figure 3B). No increase in promoter

activity was noted on *RUNX1* overexpression when sites 1 and 4 were mutated. These findings are consistent with the conclusion that sites 1 and 4, but not sites 2 and 3, are functional. *RUNX1* siRNA inhibited *RAB1B* protein expression (Figure 3C) and promoter activity (Figure 3D). Overall, these findings indicate that *RAB1B* is regulated by *RUNX1*.

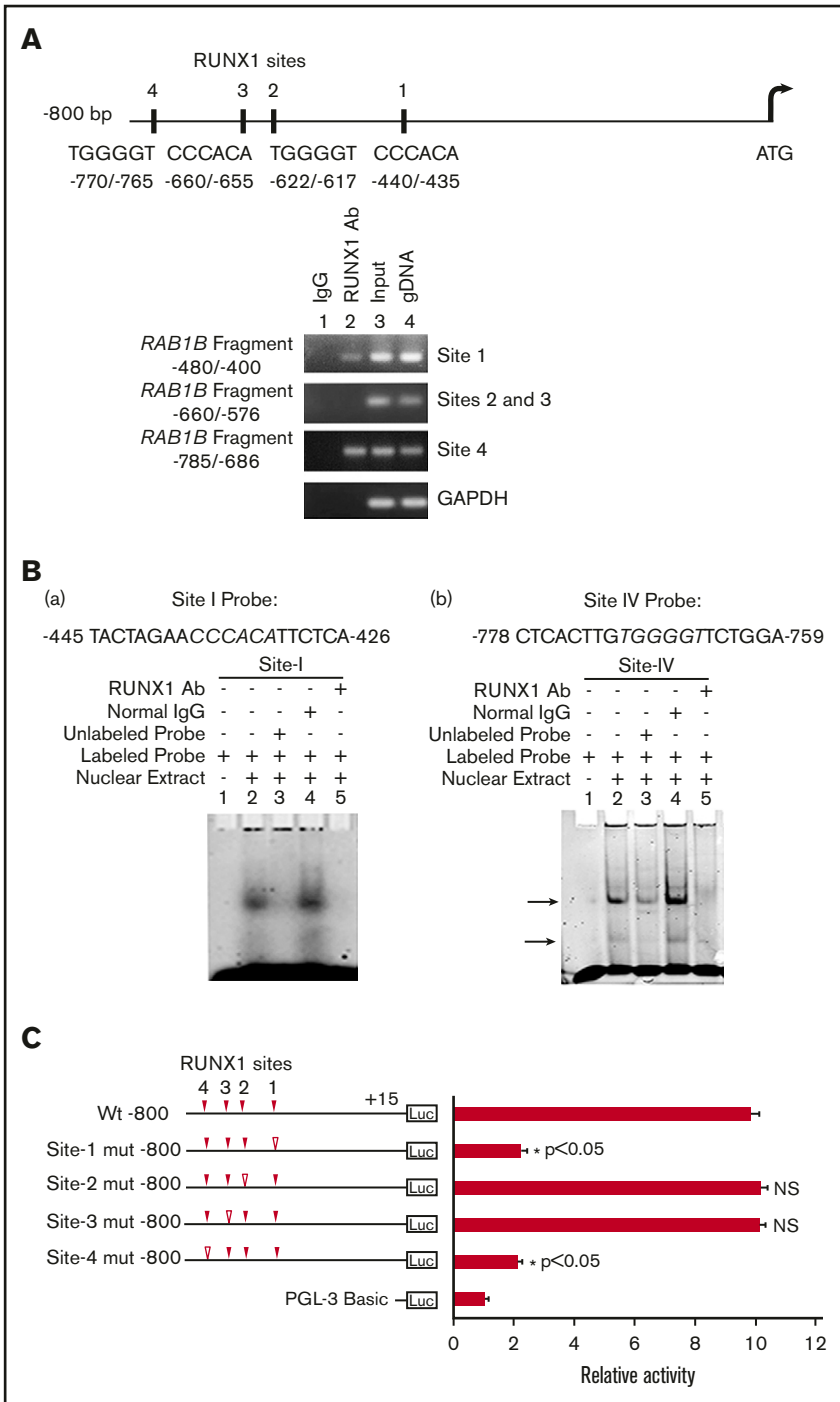
### ***RUNX1* downregulation impairs *RAB1B*-related ER-to-Golgi trafficking**

We investigated effects of *RUNX1* downregulation on ER-to-Golgi transport in megakaryocytic HEL cells. *RUNX1* downregulation revealed impaired ER-to-Golgi trafficking and dissolution of Golgi (Figure 4). HEL cells were cotransfected with vesicle protein



**Figure 2. Characterization of RUNX1 sites in the *RAB1B* upstream region.**

(A) *RAB1B* upstream region showing 4 consensus sites for RUNX1. Shown below is PCR amplification of the immunoprecipitates of HEL cells with control IgG (lane 1) and RUNX1 antibodies (lane 2). Amplification of the input or total DNA (lane 3) and genomic DNA (gDNA, lane 4) served as positive controls. Samples were analyzed by PCR using primers for the *RAB1B* region and *GAPDH*. Shown are representative of 3 experiments. (B) EMSA using WT nucleotide probes encompassing RUNX1 consensus site 1 (–426/–445; left) and site 4 (–759/–778; right) in *RAB1B* promoter and nuclear extracts from PMA-treated HEL cells. (a, left) EMSA using site 1 probe (lanes 1-5): lane 1, no extract; lane 2, protein binding to the probe; lane 3, loss of binding by competition with unlabeled probe; lane 4, no loss of binding by competition with normal IgG; and lane 5 competition with RUNX1 antibody and inhibition of binding. (b, right) EMSA using probe with site 4 (lanes 1-5); similar results were obtained as with the probe with site 1. Shown are representative of 3 experiments. (C) Luciferase reporter studies on *RAB1B* promoter in PMA-treated HEL cells. Luciferase activity with WT construct with RUNX1 sites 1-4 (solid triangles) and constructs with RUNX1 binding sites mutated (open triangles). Mutations in the sites 1 and 4 decreased promoter activity, but not the mutations in the sites 3 and 4, suggesting sites 1 and 4 are functional. The mean ± SEM is shown for 3 independent experiments in triplicates. *P* values are for comparisons against WT promoter.



VSVG-GFP and Golgi marker E2-Crimson GalT, along with scrambled control or *RUNX1* siRNA, followed by temperature shift assay to drive synchronous ER-to-Golgi transport of VSVG-GFP.<sup>21</sup> In control siRNA-transfected cells, most of the VSVG-GFP colocalized with GalT (Pearson's correlation coefficient [*r*] = 0.609 ± 0.035), indicating accumulation of VSVG in Golgi structures. On *RUNX1* knockdown, VSVG colocalization with GalT was lost (*r* = 0.378 ± 0.033; *P* < .05), and Golgi structures were disrupted (Figure 4A-B). Identical results were

obtained on downregulation of *RAB1B* (Figure 4A-B), with loss of colocalization with GalT (*r* = 0.374 ± 0.026; *P* < .05). Reconstitution of *RAB1B* in *RUNX1*-depleted cells restored the Golgi apparatus and the colocalization of VSVG (*r* = 0.711 ± 0.046; no significant difference compared with control; Figure 4B). In Figure 4C, the immunoblots show the corresponding protein levels of the *RUNX1*, *RAB1B*, and actin in control cells, with siRNA knockdown of *RUNX1* or *RAB1B*, and after ectopic expression of *RAB1B* in *RUNX1*-depleted cells. In control experiments,

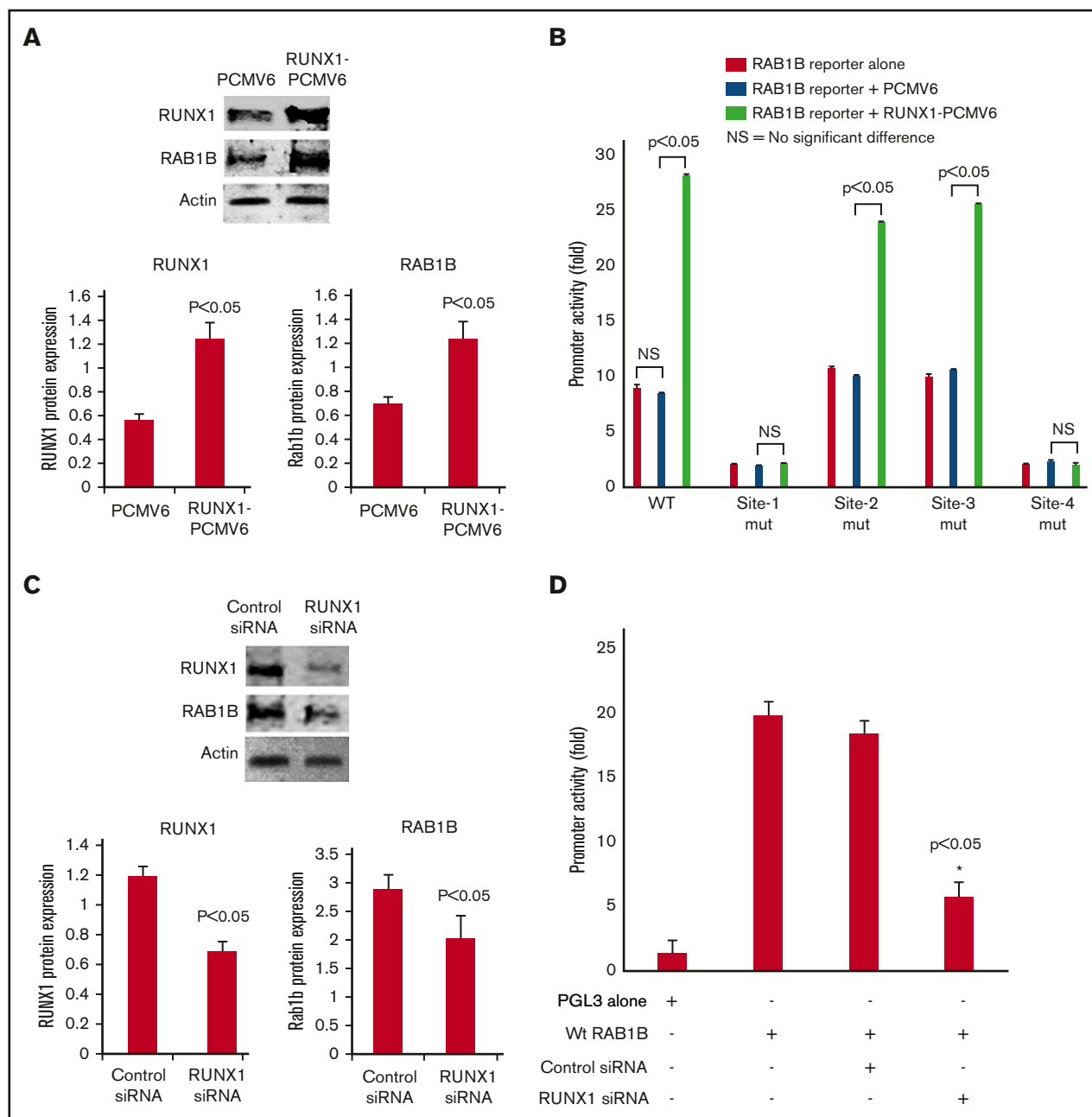


**Figure 3. Effect of *RUNX1* overexpression and *RUNX1* siRNA downregulation on *RAB1B* protein expression and promoter activity.** (A) Immunoblot analysis of *RUNX1*, *RAB1B*, and actin on overexpression of *RUNX1* in HEL cells. Bars shown are an average of 3 independent experiments. *P* values shown are for comparison with control (pCMV6 vector alone). (B) Effect of *RUNX1* overexpression on *RAB1B* promoter activity. WT construct and mutant constructs with sites 1-4 individually mutated were cotransfected with *RUNX1*-pCMV6 expression vector (green bars), empty vector pCMV6 (blue bars), or neither (red bars) in HEL cells. Reporter activity was measured at 48 hours. Bar graphs show activity as mean  $\pm$  SE of 3 independent experiments in triplicate. (C) Immunoblot analysis of lysates from HEL cells transfected with *RUNX1* siRNA showing inhibition of *RAB1B* protein. Bars shown are average of 3 independent experiments. *P* values are for comparison with control vector. (D) Effect of *RUNX1* siRNA on *RAB1B* promoter activity. *RAB1B* WT promoter construct was cotransfected with control siRNA or *RUNX1* siRNA in HEL cells. Reporter activity was measured at 48 hours. Bar graphs show activity as mean  $\pm$  SEM of 3 independent experiments in triplicate. *RUNX1* siRNA reduced *RAB1B* protein and *RAB1B* promoter activity.

*RAB1B* knockdown decreased transcript levels of *RAB1B*, but not *RAB1A* (supplemental Figure 1). Together, these studies indicate that in megakaryocytic cells, loss of *RAB1B* impairs ER-to-Golgi vesicular transport and Golgi stability, which was also noted with *RUNX1* downregulation (Figure 4). The similarity in

the effects with *RAB1B* and *RUNX1* knockdown on vesicle transport and Golgi stability, and their reversal with *RAB1B* reconstitution, suggests that *RAB1B* downregulation is the cause of the impaired ER-to-Golgi transport noted on *RUNX1* downregulation.

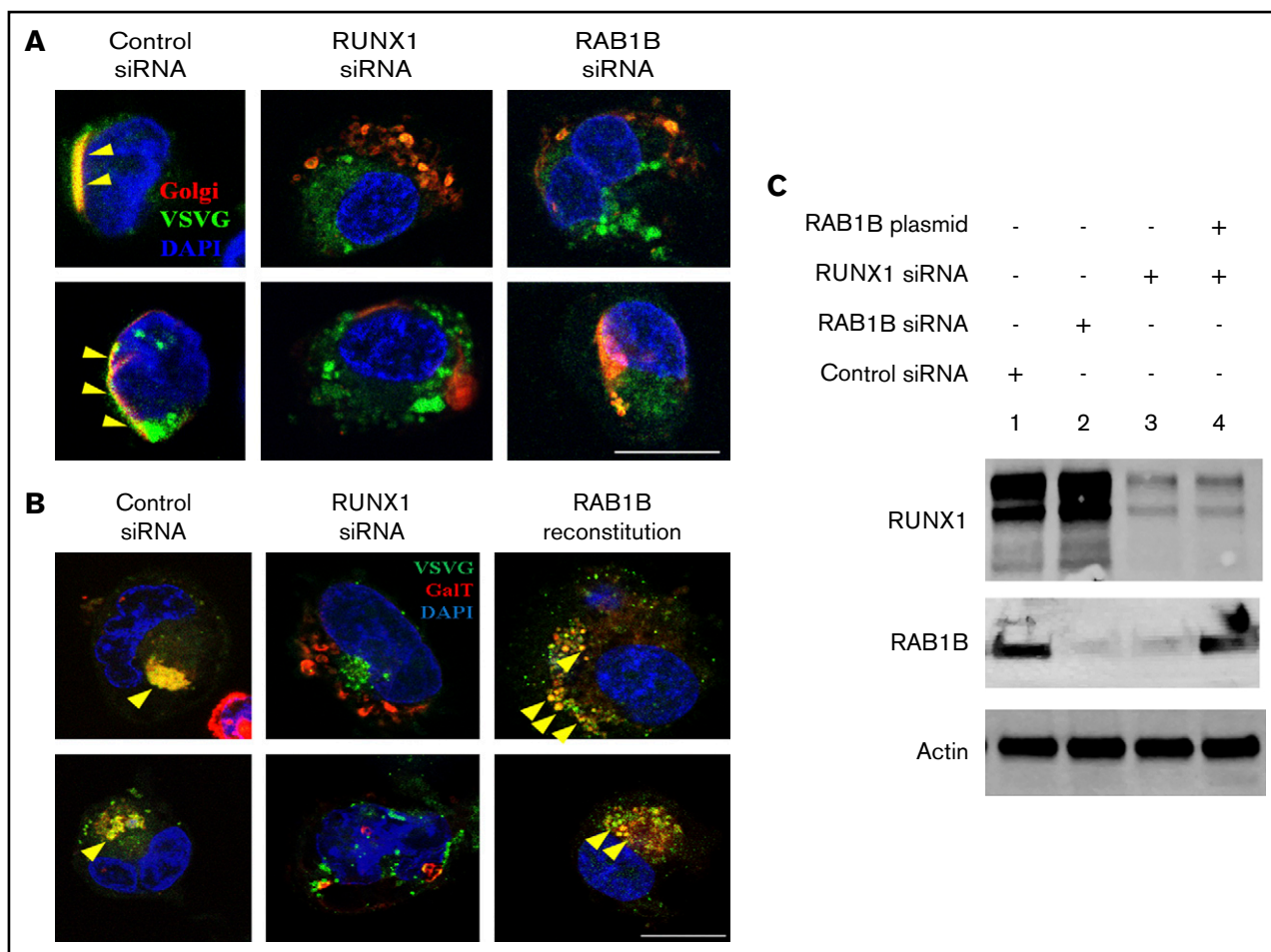


**Figure 4. Regulation of ER-to-Golgi transport by RUNX1 and RAB1B in HEL cells.** (A) PMA-treated HEL cells cotransfected with VSVG-GFP and E2 Crimson-GaIT, along with siRNAs and plasmid constructs as indicated, were seeded on coverslips, kept at 40°C for 16 hours, and then transferred to 32°C for 30 minutes and fixed. VSVG, green; GaIT, red; DAPI, blue. Yellow arrowheads indicate areas of VSVG in Golgi structures, indicated by colocalization with GaIT, which appears as yellow. Bar, 10  $\mu$ m. VSVG and GaIT were colocalized intact in the cells transfected with control siRNA (Pearson's correlation coefficient  $r = 0.609 \pm 0.035$ ; mean  $\pm$  SEM). In cells transfected with *RUNX1* siRNA ( $r = 0.378 \pm 0.033$ ;  $P < .05$ ) or *RAB1B* siRNA ( $r = 0.374 \pm 0.026$ ;  $P < .05$ ), Golgi was disrupted and there was no accumulation of VSVG-GFP, as *RAB1B* facilitates VSVG transport. (B) Resumption of VSVG transport by reconstituted *RAB1B* in HEL cells after *RUNX1* siRNA downregulation ( $r = 0.711 \pm 0.046$ ;  $P = NS$  compared with control). Bar, 10  $\mu$ m. (C) Immunoblot analysis showing reconstitution of *RAB1B* protein by ectopic *RAB1B* expression in *RUNX1*-depleted HEL cells.

### **RUNX1 downregulation impairs RAB1B-related VWF trafficking**

MK synthesize vWF, a protein present in platelet  $\alpha$ -granules, and several  $\alpha$ -granule proteins are decreased in patients with *RUNX1* haplodeficiency.<sup>4</sup> vWF is synthesized and dimerized in the ER with multimer formation occurring in the trans- and post-Golgi compartments<sup>23,24</sup> before being localized to the  $\alpha$ -granules. We postulated that vWF trafficking would be impaired because of Golgi disruption by *RUNX1* or *RAB1B* depletion, leading to defective vWF protein maturation and decreased vWF in granules. In studies performed with temperature shift as described in "Patients and methods," vWF localized to compact Golgi structures, as indicated by colocalization with GaIT in control siRNA-transfected cells (Pearson correlation coefficient  $r = 0.793 \pm 0.018$ ; Figure 5A). On *RUNX1* knockdown, the vWF concentration in the Golgi was lost ( $r = 0.478 \pm 0.072$ ;  $P < .05$ ), associated with disrupted Golgi structures (Figure 5A). Identical results were obtained on downregulation of

*RAB1B* ( $r = 0.429 \pm 0.082$ ;  $P < .05$ ). With ectopic *RAB1B* expression in *RUNX1*-depleted cells, Golgi structures were restored associated with enrichment of vWF in the Golgi ( $r = 0.665 \pm 0.048$ ; no significant difference compared with control). On immunoblot analysis, bands were strikingly decreased on downregulation of *RAB1B* (lane 2) or *RUNX1* (lane 3). Ectopic *RAB1B* expression in *RUNX1*-depleted cells partially reconstituted the vWF bands (lane 4). These findings suggest that vWF trafficking in HEL cells is regulated by *RAB1B*, and that it is impaired with *RUNX1* downregulation. In line with these findings, immunoblotting of platelet lysates from patients with *RUNX1* haplodeficiency showed that VWF was decreased relative to platelets from normal donors (Figure 5C).

### **Discussion**

These studies provide the first evidence that platelet *RAB1B* expression is downregulated in patients with *RUNX1* mutation

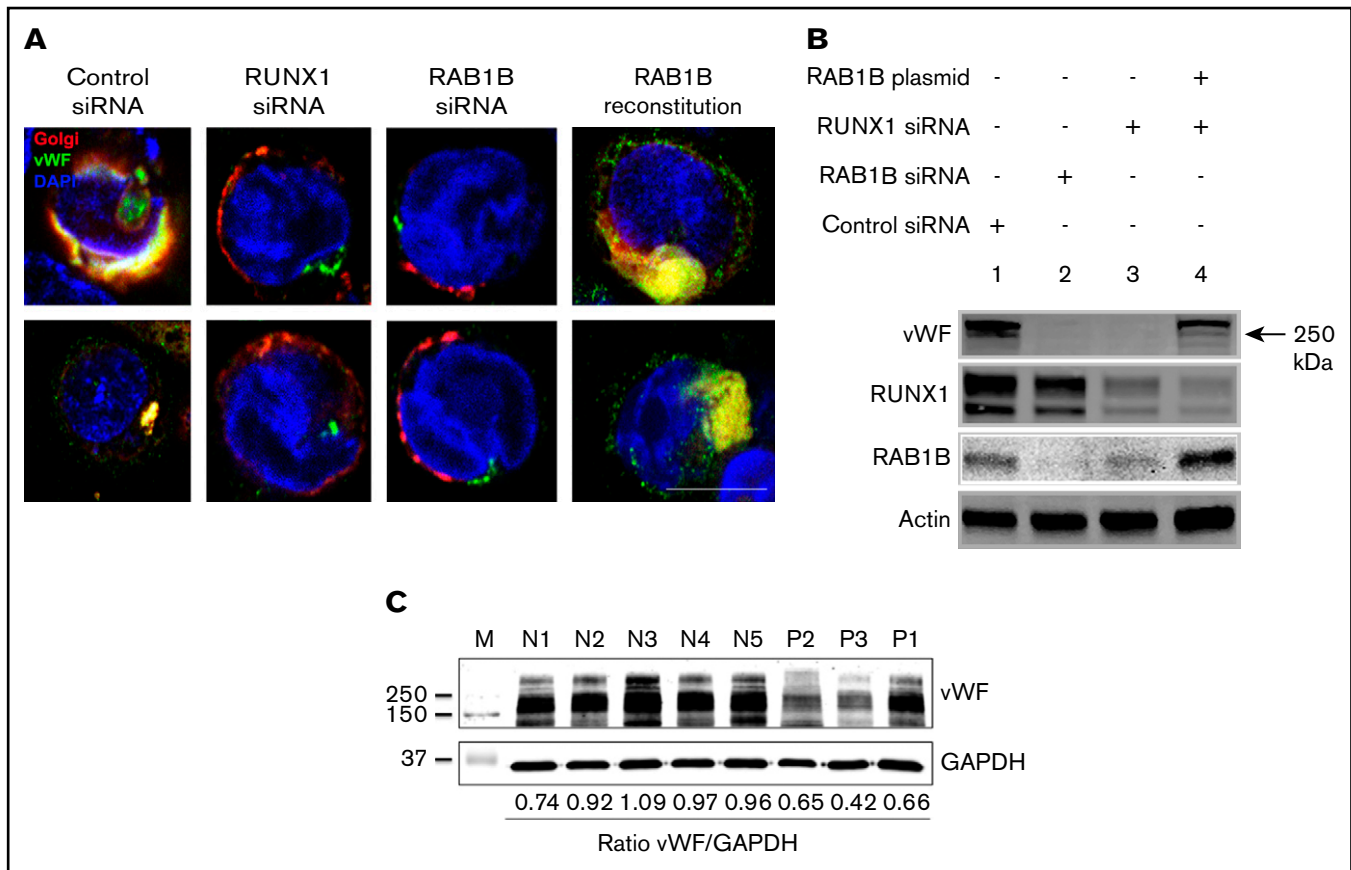


**Figure 5. Effect of siRNA depletion of *RAB1B* and *RUNX1* on vWF trafficking in HEL cells.** (A) PMA-treated HEL cells were transfected with siRNAs and expression plasmid, as indicated and as described in the legend for Figure 4. In control siRNA-transfected cells, vWF (green) colocalized with the Golgi (E2-Crimson-GalT, red; Pearson correlation coefficient  $r = 0.793 \pm 0.018$ ). On treatment with *RUNX1* siRNA ( $r = 0.478 \pm 0.072$ ;  $P < .05$ ; compared with control) or *RAB1B* siRNA ( $r = 0.429 \pm 0.082$ ;  $P < .05$ ), Golgi structures were disrupted and the colocalization with vWF was lost. *RAB1B* expression in *RUNX1* siRNA-depleted cells reconstituted the Golgi structures along with colocalization of vWF ( $r = 0.665 \pm 0.082$ ;  $P = \text{NS}$ ), similar to that seen in control cells. Bar, 10  $\mu\text{m}$ . (B) Immunoblot analysis of vWF, RUNX1, RAB1B, and actin in HEL cells treated as described earlier. Downregulation of *RAB1B* or *RUNX1* decreased vWF; reconstitution of *RAB1B* in *RUNX1*-depleted cells restored the vWF. (C) Platelet vWF by immunoblotting in 3 patients with *RUNX1* mutations and 5 normal subjects. Also shown is the ratio of vWF to GAPDH as loading control.

(Figure 1), and that *RAB1B* is regulated in megakaryocytic HEL cells by RUNX1 (Figures 2 and 3). The latter provides a mechanism for the decreased platelet *RAB1B* in patients with *RUNX1* haplodeficiency. Rab proteins regulate specific steps in vesicle transport in the secretory and endocytic pathways, and this is driven by their cellular locations.<sup>18</sup> *RAB1B* has been shown in HeLa cells<sup>14,15,17</sup> and CHO cells<sup>16</sup> to regulate ER-to-Golgi vesicle transport,<sup>17,21,25</sup> and loss of *RAB1B* expression resulted in decreased ER-to-Golgi vesicle trafficking with disruption of Golgi. However, cell biological roles of *RAB1B* in MK cells have not been explored. Moreover, HeLa cells do not express RUNX1.<sup>19</sup> Our studies provide the first evidence that *RAB1B* regulates ER-to-Golgi vesicle transport in megakaryocytic cells. *RAB1B* downregulation impaired ER-to-Golgi vesicle trafficking and induced Golgi dissolution (Figure 4). Identical findings were observed on *RUNX1* downregulation with reversal of the findings on ectopic expression of *RAB1B* in *RUNX1*-depleted cells (Figures 4B and 5), indicating that the defective ER-to-Golgi transport with *RUNX1* downregulation was secondary to decreased *RAB1B* expression. This does not exclude a contributory effect of other genes also downregulated in *RUNX1* haplodeficiency.<sup>7</sup>

ER-to-Golgi trafficking is a critical and early step in the transport of proteins synthesized in the ER to the specific granules.<sup>26-28</sup> Defect in granule number or content (of both  $\alpha$  and dense granules) is a hallmark of *RUNX1* haplodeficiency.<sup>4</sup> Platelet  $\alpha$ -granules are endowed with numerous proteins, many, but not all, of which are synthesized in the MK. Deficiencies of  $\alpha$ -granule proteins such as platelet factor-4 and  $\beta$ -thromboglobulin have been documented in patients with *RUNX1* mutations.<sup>4,11</sup> We show that vWF is also decreased. In MK, small vesicles budding from the trans-Golgi network are transported from MK to pro-platelets via multivesicular bodies.<sup>26-28</sup> Multiple mechanisms contribute to the handling and trafficking of various proteins to specific platelet granules. We postulate that impaired ER-to-Golgi transport resulting from decreased *RAB1B* expression (arising from *RUNX1* mutations) is an important mechanism causing defective protein cargo trafficking early in the process that leads to granule biogenesis in *RUNX1* haplodeficiency, particularly for  $\alpha$ -granule proteins that are synthesized in the MK.

Our studies show that *RUNX1* or *RAB1B* downregulation impairs handling of vWF (Figure 5), a protein synthesized by MK and present in  $\alpha$ -granules. Several RAB proteins, but not *RAB1B*, to our knowledge,



have been implicated in the handling of vWF in endothelial cells.<sup>29</sup> Our studies implicate RAB1B in vWF trafficking in megakaryocytic HEL cells (Figure 5A). The lack of full reconstitution of vWF on RAB1B re-expression in RUNX1-depleted cells is consistent with the conclusion that RAB1B is necessary, but not sufficient, to normalize vWF trafficking. This may be related to other genes also being downregulated with RUNX1 downregulation.<sup>7</sup> In line with these findings, platelet vWF was decreased in patients with RUNX1 mutations (Figure 5C). Of note, in our patient, the platelet vWF transcript level was not decreased on expression profiling,<sup>7</sup> the latter being the reason for selecting vWF for the studies on RAB1B-regulated protein trafficking. In addition, plasma vWF was normal, suggesting a differential regulation of vWF between MK and endothelial cells. These findings are in line with the conclusion that the abnormal platelet/MK $\alpha$ -granule vWF in RUNX1 haplodeficiency results from downregulation of genes involved in protein trafficking in MK, rather than RUNX1 regulation of the vWF gene.

Impaired roles of RAB proteins, specifically RAB1B, have been recognized in some human neurodegenerative diseases: Alzheimer's disease<sup>30,31</sup> and Parkinson's disease.<sup>32,33</sup> RAB1B regulates transport of  $\beta$ -amyloid precursor protein from ER-to-Golgi.<sup>30,31</sup> In Parkinson's disease models,  $\alpha$ -synuclein blocks ER-to-Golgi trafficking, and RAB1 rescues the neuron loss.<sup>32,33</sup> Interestingly, Golgi fragmentation, noted in our studies (Figure 4), is also reported in neurodegenerative diseases.<sup>33</sup>

In summary, our studies show that RAB1B is regulated by transcription factor RUNX1 in megakaryocytic cells/platelets and is downregulated in platelets from RUNX1 haplodeficiency patients. RUNX1 downregulation is associated with defective ER-to-Golgi transport that is reversed, at least in part, by re-expression of RAB1B. ER-to-Golgi

transport is an important step in the trafficking of proteins synthesized in the MK to specific granules, and a defect in this process likely contributes to the defects in protein-bearing platelet  $\alpha$ -granules. These findings provide new insights into the mechanisms leading to granule deficiencies in RUNX1 haplodeficiency.

## Acknowledgments

This study was supported by research funding from National Institutes of Health, National Heart, Lung, and Blood Institute grants R01HL109568 and R01HL13736 (A.K.R.), and R01HL137207 (L.E.G.).

## Authorship

Contribution: G.J. performed the research, analyzed and interpreted data, and wrote the paper; L.E.G. designed and performed the research, analyzed and interpreted the data with respect to the immunofluorescence studies, and contributed to the writing of the manuscript; G.M. performed some of the measurements; M.P.L. performed studies in establishing the RUNX1 mutation in 2 of the patients and revised the manuscript; A.K.R. conceived, designed, and performed the research, interpreted data, and wrote the paper; and all authors have read and approved the manuscript.

Conflict-of-interest disclosure: The authors declare no competing financial interests.

ORCID profile: A.K.R., 0000-0002-3078-7778.

Correspondence: A. Koneti Rao, Sol Sherry Thrombosis Research Center, Section of Hematology, Lewis Katz School of Medicine at Temple University, 3420 N Broad St, 204 MRB, Philadelphia, PA 19140; e-mail: koneti@temple.edu.

## References

1. Sood R, Kamikubo Y, Liu P. Role of RUNX1 in hematological malignancies. *Blood*. 2017;129(15):2070-2082.
2. Bonifer C, Levantini E, Kouskoff V, Lacaud G. Runx1 structure and function in blood cell development. *Adv Exp Med Biol*. 2017;962:65-81.
3. Song WJ, Sullivan MG, Legare RD, et al. Haploinsufficiency of CBFA2 causes familial thrombocytopenia with propensity to develop acute myelogenous leukaemia. *Nat Genet*. 1999;23(2):166-175.
4. Songdej N, Rao AK. Hematopoietic transcription factor mutations: important players in inherited platelet defects. *Blood*. 2017;129(21):2873-2881.
5. de Bruijn MF, Speck NA. Core-binding factors in hematopoiesis and immune function. *Oncogene*. 2004;23(24):4238-4248.
6. Gabbeta J, Yang X, Sun L, McLane MA, Niewiarowski S, Rao AK. Abnormal inside-out signal transduction-dependent activation of glycoprotein IIb-IIIa in a patient with impaired pleckstrin phosphorylation. *Blood*. 1996;87(4):1368-1376.
7. Sun L, Gorospe JR, Hoffman EP, Rao AK. Decreased platelet expression of myosin regulatory light chain polypeptide (MYL9) and other genes with platelet dysfunction and CBFA2/RUNX1 mutation: insights from platelet expression profiling. *J Thromb Haemost*. 2007;5(1):146-154.
8. Mao GF, Goldfinger LE, Fan DC, et al. Dysregulation of PLDN (pallidin) is a mechanism for platelet dense granule deficiency in RUNX1 haplodeficiency. *J Thromb Haemost*. 2017;15(4):792-801.
9. Sun L, Mao G, Rao AK. Association of CBFA2 mutation with decreased platelet PKC- $\theta$  and impaired receptor-mediated activation of GPIIb-IIIa and pleckstrin phosphorylation: proteins regulated by CBFA2 play a role in GPIIb-IIIa activation. *Blood*. 2004;103(3):948-954.
10. Jalagadugula G, Mao G, Kaur G, Goldfinger LE, Dhanasekaran DN, Rao AK. Regulation of platelet myosin light chain (MYL9) by RUNX1: implications for thrombocytopenia and platelet dysfunction in RUNX1 haplodeficiency. *Blood*. 2010;116(26):6037-6045.
11. Aneja K, Jalagadugula G, Mao G, Singh A, Rao AK. Mechanism of platelet factor 4 (PF4) deficiency with RUNX1 haplodeficiency: RUNX1 is a transcriptional regulator of PF4. *J Thromb Haemost*. 2011;9(2):383-391.
12. Jalagadugula G, Mao G, Kaur G, Dhanasekaran DN, Rao AK. Platelet protein kinase C- $\theta$  deficiency with human RUNX1 mutation: PRKCQ is a transcriptional target of RUNX1. *Arterioscler Thromb Vasc Biol*. 2011;31(4):921-927.
13. Kaur G, Jalagadugula G, Mao G, Rao AK. RUNX1/core binding factor A2 regulates platelet 12-lipoxygenase gene (ALOX12): studies in human RUNX1 haplodeficiency. *Blood*. 2010;115(15):3128-3135.

14. Martinez H, García IA, Sampieri L, Alvarez C. Spatial-temporal study of Rab1b dynamics and function at the ER-Golgi interface. *PLoS One*. 2016;11(8):e0160838.
15. Tisdale EJ, Bourne JR, Khosravi-Far R, Der CJ, Balch WE. GTP-binding mutants of rab1 and rab2 are potent inhibitors of vesicular transport from the endoplasmic reticulum to the Golgi complex. *J Cell Biol*. 1992;119(4):749-761.
16. Plutner H, Cox AD, Pind S, et al. Rab1b regulates vesicular transport between the endoplasmic reticulum and successive Golgi compartments. *J Cell Biol*. 1991;115(1):31-43.
17. Alvarez C, Garcia-Mata R, Brandon E, Sztul E. COPI recruitment is modulated by a Rab1b-dependent mechanism. *Mol Biol Cell*. 2003;14(5):2116-2127.
18. Stenmark H. Rab GTPases as coordinators of vesicle traffic. *Nat Rev Mol Cell Biol*. 2009;10(8):513-525.
19. Martinez M, Hinojosa M, Trombly D, et al. Transcriptional auto-regulation of RUNX1 P1 promoter. *PLoS One*. 2016;11(2):e0149119.
20. Jalagadugula G, Dhanasekaran DN, Kim S, Kunapuli SP, Rao AK. Early growth response transcription factor EGR-1 regulates Galphaq gene in megakaryocytic cells. *J Thromb Haemost*. 2006;4(12):2678-2686.
21. Presley JF, Cole NB, Schroer TA, Hirschberg K, Zaal KJ, Lippincott-Schwartz J. ER-to-Golgi transport visualized in living cells. *Nature*. 1997;389(6646):81-85.
22. Wurtzel JG, Kumar P, Goldfinger LE. Palmitoylation regulates vesicular trafficking of R-Ras to membrane ruffles and effects on ruffling and cell spreading. *Small GTPases*. 2012;3(3):139-153.
23. Wagner DD. Cell biology of von Willebrand factor. *Annu Rev Cell Biol*. 1990;6(1):217-246.
24. de Wit TR, van Mourik JA. Biosynthesis, processing and secretion of von Willebrand factor: biological implications. *Best Pract Res Clin Haematol*. 2001;14(2):241-255.
25. García IA, Martínez HE, Alvarez C. Rab1b regulates COPI and COPII dynamics in mammalian cells. *Cell Logist*. 2011;1(4):159-163.
26. Heijnen HF, Debili N, Vainchencker W, Breton-Gorius J, Geuze HJ, Sixma JJ. Multivesicular bodies are an intermediate stage in the formation of platelet alpha-granules. *Blood*. 1998;91(7):2313-2325.
27. Youssefian T, Cramer EM. Megakaryocyte dense granule components are sorted in multivesicular bodies. *Blood*. 2000;95(12):4004-4007.
28. Richardson JL, Shivdasani RA, Boers C, Hartwig JH, Italiano JE Jr. Mechanisms of organelle transport and capture along proplatelets during platelet production. *Blood*. 2005;106(13):4066-4075.
29. Nightingale T, Cutler D. The secretion of von Willebrand factor from endothelial cells; an increasingly complicated story. *J Thromb Haemost*. 2013;11(Suppl 1):192-201.
30. Jiang S, Li Y, Zhang X, Bu G, Xu H, Zhang YW. Trafficking regulation of proteins in Alzheimer's disease. *Mol Neurodegener*. 2014;9(1):6.
31. Dugan JM, deWit C, McConlogue L, Maltese WA. The Ras-related GTP-binding protein, Rab1B, regulates early steps in exocytic transport and processing of beta-amyloid precursor protein. *J Biol Chem*. 1995;270(18):10982-10989.
32. Cooper AA, Gitler AD, Cashikar A, et al. Alpha-synuclein blocks ER-Golgi traffic and Rab1 rescues neuron loss in Parkinson's models. *Science*. 2006;313(5785):324-328.
33. Rendón WO, Martínez-Alonso E, Tomás M, Martínez-Martínez N, Martínez-Menárguez JA. Golgi fragmentation is Rab and SNARE dependent in cellular models of Parkinson's disease. *Histochem Cell Biol*. 2013;139(5):671-684.